Supporting Information

Syed et al. 10.1073/pnas.1003292107

SI Text

1. Comparison of Global-Ocean Mass Change ($\Delta M/\Delta t$) Estimates: 2003–2006. In order to validate the estimated ocean mass changes ($\Delta M_{\mathrm{ISHII}}/\Delta t$ and $\Delta M_{\mathrm{IH}}/\Delta t$) for the period of 2003–2006, we have computed ancillary estimates of ΔM utilizing the ARGO array of temperature and salinity profiling floats (www.argo.ucsd.edu) and Gravity Recovery and Climate Experiment (GRACE) observations. While the ARGO-based ocean mass changes ($\Delta M_{\mathrm{ARGO}}/\Delta t$) are determined by removing ARGO-based steric contributions from altimeter-based global mean sea level (GMSL) variations, GRACE data provides the first direct observation of global ocean mass change (1). Unlike the Ingleby and Huddleston (2) (IH) dataset, Ishii et al. (3) (ISHII) data did not include observations of monthly ocean salinity with depth. Hence, the salinity data required for the computation of M_{ISHII} was obtained from the recent *World Ocean Atlas 2005* climatology grids (4). However, it is important to note that the salinity-driven changes in global steric sea surface height are negligible compared to those driven by changes in temperature and are moreover invariant in time (5, 6). Because these validation datasets are available only beyond 2003, the comparison of our longer time series of monthly estimates of global ocean mass changes ($\Delta M_{\mathrm{ISHII}}/\Delta t$ and $\Delta M_{\mathrm{IH}}/\Delta t$) shown in Fig. S2 is restricted to the common period of 2003–2006. Comparison of month-to-month variability in $\Delta M_{\mathrm{ISHII}}/\Delta t$ and $\Delta M_{\mathrm{IH}}/\Delta t$ reveals very good agreement with direct measurements from GRACE [correlation coefficient $(R) > 0.85$, $p < 0.01$] and $\Delta M_{\mathrm{ARGO}}/\Delta t$ ($R > 0.92$, $p < 0.01$). Global ocean mass change peaks during Northern Hemisphere summer, corresponding to the peak in global discharge (7, 8).

2. Comparison of Global-Ocean Evaporation (E) Estimates. Monthly variability of E estimates from different sources is shown in Fig. S5. Although Objectively Analyzed Air-Sea Fluxes (OAFlux) estimates are higher (lower) than Hamburg Ocean Atmosphere Parameters and Fluxes from Satellite data (HOAPS) before (after) 2001, their average over the study period (1994–2006), 415,890 km^3/y and 410,640 km^3/y, respectively, are quite comparable and commensurate with previous studies (9, 10). In contrast, Special Sensor Microwave Imager (SSM/I) estimates are noted to be coherently lower (400,240 km^3/y) than either of HOAPS and OAFlux, even though both these datasets include SSM/I retrievals in their analysis. These differences can be attributed to the fact that each of these estimates differs in the way each synthesizes in situ observations, ship reports, reanalysis products, and different satellite retrievals to improve their results.

1. Chambers DP (2006) Evaluation of new GRACE time-variable gravity data over the ocean. *Geophys Res Lett* 33:L17603.
2. Ingleby B, Huddleston M (2007) Quality control of ocean temperature and salinity profiles—Historical and real-time data. *J Marine Syst* 65:158–175.
3. Ishii M, Kimoto M, Sakamoto K, Iwasaki SI (2006) Steric sea level changes estimated from historical ocean subsurface temperature and salinity analyses. *J Oceanogr* 62:155–170.
4. Antonov JI, et al. (2006) Salinity. *World Ocean Atlas 2005* (US Government Printing Office, Washington, DC), Vol 2, 182 pp.
5. Lombard A, et al. (2007) Estimation of steric sea level variations from combined GRACE and Jason-1 data. *Earth Planet Sci Lett* 254:194–202.
6. Willis J. K. (2009) personal communication.
7. Dai A, Trenberth KE (2002) Estimates of freshwater discharge from continents: Latitudinal and seasonal variations. *J Hydrometeorol* 3 (6):660–687.
8. Syed TH, Famiglietti JS, Chambers DP (2009) GRACE-based estimates of terrestrial freshwater discharge from basin to continental scales. *J Hydrometeorol* 10:22–40.
9. Trenberth KE, Smith L, Qian T, Dai A, Fasullo J. (2007) Estimates of the global water budget and its annual cycle using observational and model data, *J Hydrometeorol* 8:758–769.
10. Schlosser CA, Houser PR (2007) Assessing a satellite-era perspective of the global water cycle. *J Climate* 20:1316–1338.

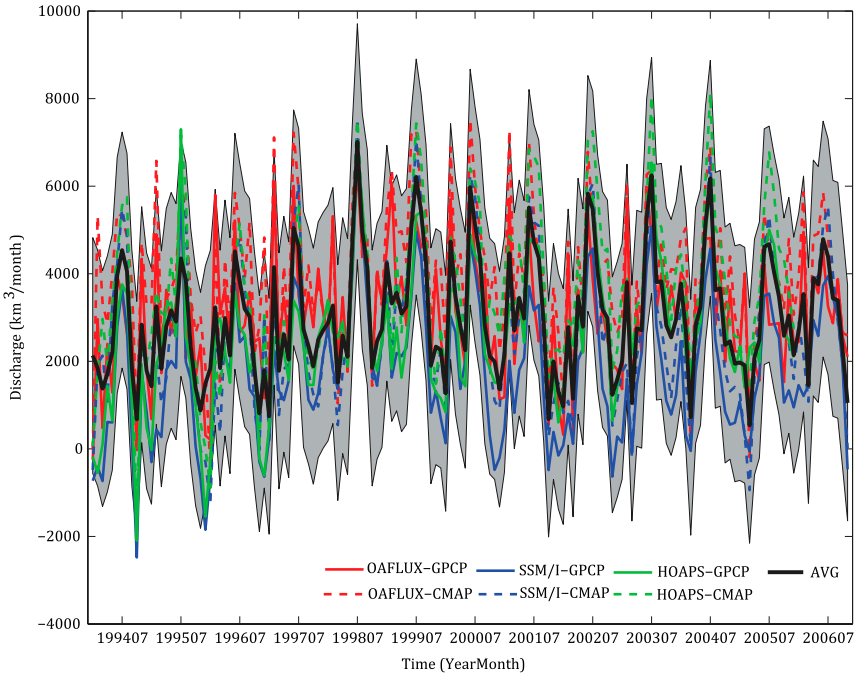

Fig. S1. Monthly time series of global freshwater discharge computed using the average of $\Delta M/\Delta t$ with combinations of P and E estimates for the period of 1994–2006. Each of the discharge estimates is referred to by the source of E and P. Evaporation from OAFlux, SSM/I, and HOAPS is represented by red, blue, and green lines, respectively. Likewise, precipitation from Global Precipitation and Climatology Project (GPCP) and Climate Prediction Center (CPC) Merged Analysis of Precipitation (CMAP) is denoted with solid and broken lines, respectively. Hence discharge estimates using E from OAFlux and P from GPCP are shown as a solid red line (OAFlux-GPCP) and that of OAFlux and CMAP as a broken red line (OAFlux-CMAP). The ensemble mean of the various freshwater discharge estimates is represented by the solid black line, and the shaded (gray) portion represents ± 1 standard deviation of the ensemble mean (68% confidence interval).

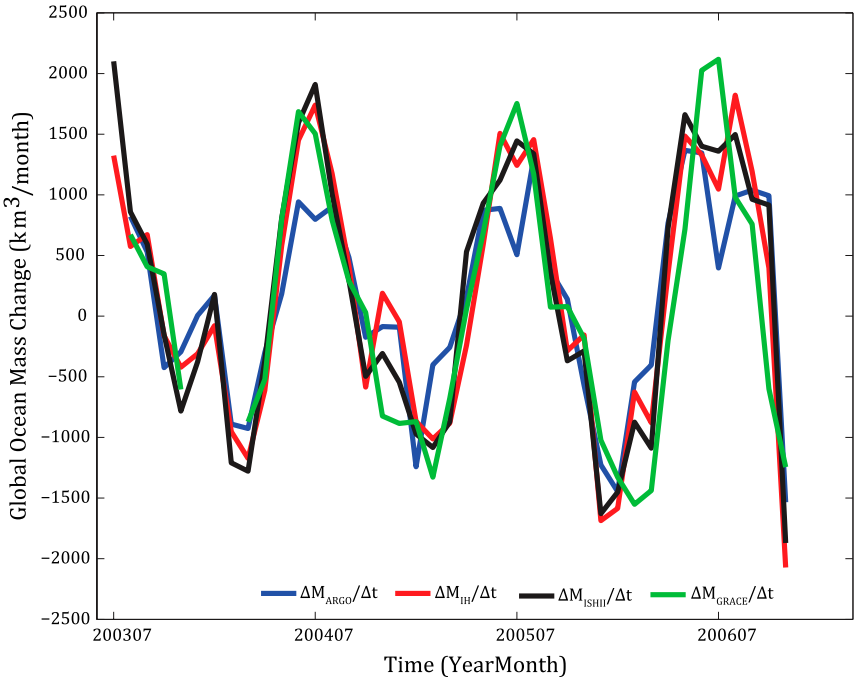

Fig. S2. Monthly time series of global ocean mass changes are computed utilizing altimeter GMSL measurements with IHSII ($\Delta M_{\mathrm{ISHII}}/\Delta t$; black), IH ($\Delta M_{\mathrm{IH}}/\Delta t$; red), and ARGO ($\Delta M_{\mathrm{ARGO}}/\Delta t$; blue). Also shown are the direct measurements of $\Delta M/\Delta t$ from GRACE ($\Delta M_{\mathrm{GRACE}}/\Delta t$; green) for the period of 2003–2006. Consistent discrepancies are evident in the peaks of global-ocean mass changes, around the month of July. A dip in $\Delta M_{\mathrm{ARGO}}/\Delta t$ is evident during the months of July, but is less apparent in $\Delta M_{\mathrm{ISHII}}/\Delta t$ and $\Delta M_{\mathrm{IH}}/\Delta t$ and is absent in the GRACE-based estimates. However, with time, an increasing number of ARGO profiles are incorporated in the ISHII and IH datasets so that peaks in $\Delta M_{\mathrm{ISHII}}/\Delta t$ and $\Delta M_{\mathrm{IH}}/\Delta t$ become progressively closer to those of $\Delta M_{\mathrm{ARGO}}/\Delta t$.

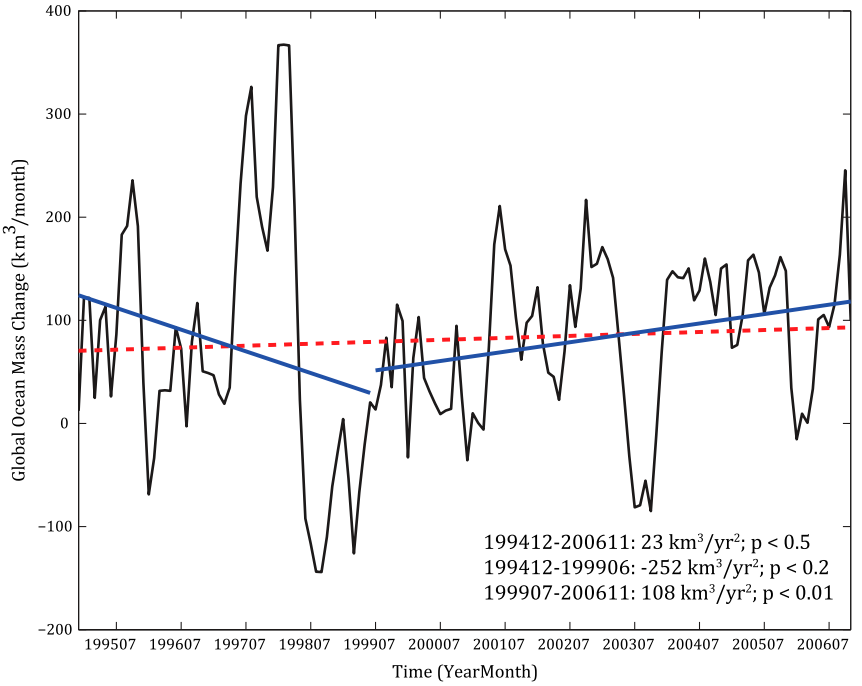

Fig. S3. Monthly time series of global-ocean mass change ($\Delta M/\Delta t$) smoothed with a 12-month moving average filter. Also shown are the emerging (short-term) trends, estimated as the slope of the best fit line, based on a least squares fit, for the periods of 199412–200611 (broken red line), 199412–199906 (solid blue line), and 199907–200611 (solid blue line), and their respective p values (shown in the legend). Trends in $\Delta M/\Delta t$ actually represent acceleration in global-ocean water mass. Note that contributions from the Greenland and Antarctic ice sheet, alpine glaciers, and other land-management practices (e.g., reservoir storage and groundwater mining) are implicitly included in this trend.

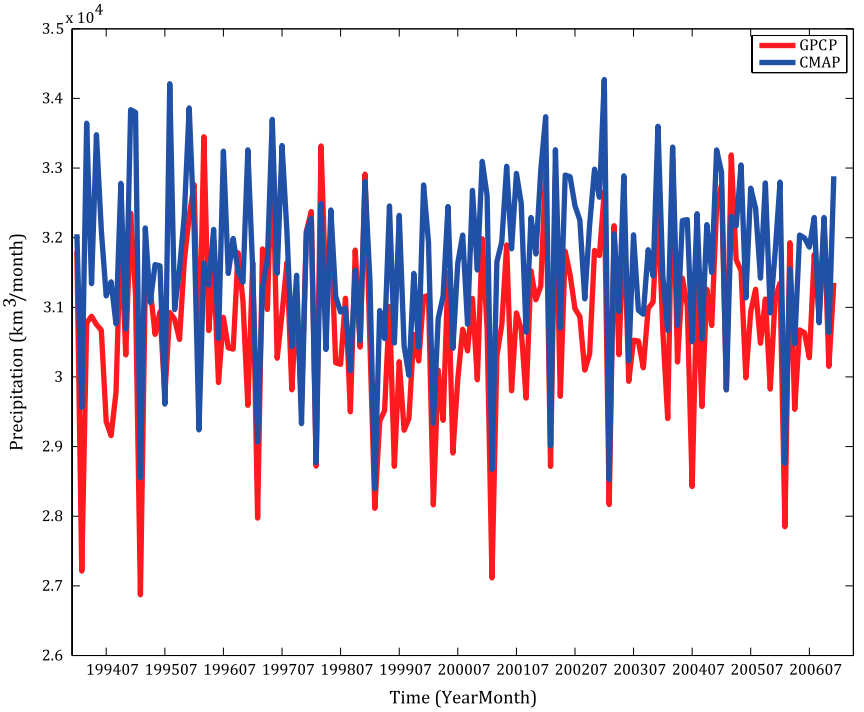

Fig. S4. Month-to-month variations of global ocean precipitation estimated from GPCP (red) and CMAP (blue) for the period 1994–2006.

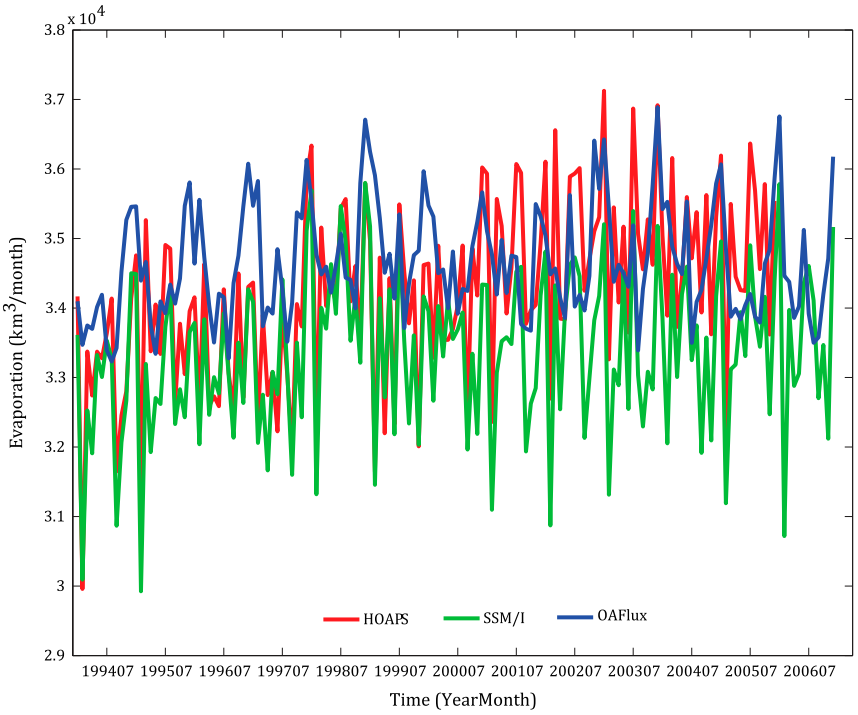

Fig. S5. A comparison of global ocean evaporation estimates obtained from HOAPS (red), SSM/I (green), and OAFlux (blue) for the period 1994–2006.

Table S1. Estimated emerging (short-term) trends in global freshwater discharge

Data source	Trend, km^3/y^2	*p* value
OAFlux-CMAP	−59	0.65
OAFlux-GPCP	85	0.52
SSM/I-CMAP	333	0.02
SSM/I-GPCP	475	<0.001
HOAPS-CMAP	1764	0
HOAPS-CMAP	1899	0
Avg	540	<0.001

The trends are from all combinations of *P* and *E* datasets, including the ensemble mean (avg), for the entire study period (1994–2006). The significance of the estimated trend is given by the *p* values obtained in each case.